

EFFECTS OF FRACTIONAL WETTABILITY AND ITS SPATIAL HETEROGENEITY ON THE CAPILLARY PRESSURE AND RELATIVE PERMEABILITY FUNCTIONS

Varvara Sygouni^{1,2}, Christos D. Tsakiroglou^{1,*}, Alkiviades C. Payatakes^{1,2}

¹FORTH / ICE-HT, Stadiou Street, Platani, P.O. Box 1414, GR – 26504 Patras, Greece

²Department of Chemical Engineering, University of Patras, GR – 26504 Patras, Greece

This paper was prepared for presentation at the International Symposium of the Society of Core Analysts held in Toronto, Canada, 21-25 August, 2005

ABSTRACT

A model porous medium of controlled fractional wettability is fabricated by mixing intermediate-wet glass microspheres with oil-wet PTFE microspheres, and packing them between two transparent glass plates. Visualization experiments of the displacement of an oleic by an aqueous phase are performed on the model porous medium at very low flow rates for the system: silicon oil / distilled water colored with methylene blue. The displacement is dominated by capillary forces, and the transient growth pattern is the result of various classes of flow events that are strongly correlated with the observed fluctuations of the pressure drop. The measured pressure drop of each displacement is analyzed with wavelets and is transformed to a capillary pressure spectrum which enables us to identify the position, amplitude, and width of the most important fluctuations. The falls of the capillary pressure may be correlated with a local wettability factor, presuming that they refer to identical flow events of the displacement. The average pre-breakthrough capillary pressure is a linearly increasing function of the fraction of the oil-wet solid particles. The non-random distribution of heterogeneous wettability is the driving force for the discontinuous production of oil pockets after the water breakthrough, whereas the post-breakthrough sharp fluctuations of the pressure drop indicate variation of the average capillary resistance arising from fluid redistribution between areas of different wettability.

INTRODUCTION

The wettability of porous media with respect to a fluid system plays an important role in a variety of multiphase flow processes of industrial and environmental interest (enhanced oil recovery, soil contamination and remediation, drying, wetting, etc.) [10,12,14]. The wettability expresses the affinity of a surface for water or oil, and is governed by the interaction of short range surface forces [6]. The spatial variation of the surface forces

* Corresponding author, e-mail: ctsakir@iceht.forth.gr, Tel.: 2610 965212, Fax: 2610 965223

over the porous formation may lead to conditions of heterogeneous (fractional, mixed) wettability [1].

In reservoir engineering, the wettability of porous rocks is commonly quantified by the Amott, Amott-Harvey and USBM macroscopic indices [1,11]. However, these indices are complex functions of the pore size distribution, pore space connectivity and wettability [4], and are unable to inform us explicitly about the spatial distribution and relative percentage of the oil-wet and water-wet pore surface in a fractional-wet porous medium. A great variety of models and theoretical simulators have been developed to interpret the dependence of the two- and three-phase flow coefficients of porous media on the fractional/mixed wettability [3,4,7,8,12].

Advanced techniques, such as the analysis of NMR relaxation times can give only qualitative information concerning the creation of conditions of mixed wettability in a porous medium [5,9]. The displacement front could also be used to quantify the effect of wettability on the displacement process [2]. The transient response of the pressure drop across a pore network is a “fingerprint” of the dominated flow pattern [13]. Successive fluctuations of the capillary pressure are associated with the variability of pore sizes and may be employed to get information concerning the pore space geometry from data of rate-controlled porosimetry [15].

The final objective of the present work is to suggest a procedure for analyzing the results of unsteady displacement experiments performed on porous samples and extracting quantitative information concerning the distribution of fractional wettability over the solid surface of a porous medium. Visualization immiscible displacement experiments are performed at very low values of the capillary number on a two-layer model porous medium consisting of pores of identical size and controlled fractional wettability. The spatial variation of wettability is correlated with the transient displacement pattern, and the fluctuations of the pressure drop which are analyzed with the aid of wavelets.

METHODS AND MATERIALS

The model porous medium consists of glass and PTFE micro-spheres of identical diameter (≈ 0.15 cm) packed between a silicon rubber and two cover glass plates (Fig.1). Five holes drilled on the two ends of the upper plate serve as inlet and outlet ports. The fluids used in displacement experiments were silicon oil and deionized water colored with methylene blue (Table 1). The fractional wettability of the porous medium was adjusted by mixing intermediate-wet (iw) glass spheres with strongly oil-wet (ow) PTFE spheres at varying fractions, f_p , ranging from 0 to 1.

In a typical experiment, initially, the pore space is filled completely with the oil (defender), which is then displaced by water (invader) injected at constant influx rate through a syringe pump. With the aid of a differential pressure transducer operating over a very low pressure range (0-850 Pa), the pressure drop across the porous medium is measured every 20 s and transmitted to a data acquisition card installed in the host computer. At equal time intervals, snap-shots of the displacement are captured with a CCD camera, transmitted to an image grabber and recorded on the hard disk of the PC.

The porous medium can be regarded as a two-layer (3-dimensional) throat-and-chamber network composed of two interconnected triangular lattices. In each layer, throats are formed between two spherical particles and one cover plate, pore chambers are formed among any three particles touching each other and one of the cover plates, whereas the narrowest cross-sectional area of chambers coincides with the vertical throats interconnecting the two layers (Fig.2). It is worth noting that the pore surface is fractional-wet not only at the network scale but also at the scale of individual pores. Depending on the wetting state of the surrounding solid surface, the throats and chambers can be classified in various classes (Fig. 2).

The absolute permeability of the porous medium was measured and found $k = 1500 D$. All experiments were performed under a very low value of the capillary number ($Ca = \mu_o u / \gamma_{ow} = 1.26 \cdot 10^{-8}$) so that the viscous pressure drop across the entire porous medium was two orders of magnitude smaller than the average capillary pressure required for a meniscus to penetrate in a throat.

Wavelet Analysis

For most signals the low frequency component is of great importance and is commonly employed in the analysis of physical / chemical processes. However, information concerning the individual features of a signal is also embedded into the high frequency component. Wavelet analysis refers to approximations and details. The approximations are high scale –low frequency constituents of a signal, and the details are low scale – high frequency constituents. In all cases, the details describe fast (sharp) changes of the signal. The signal (S) passes through a low pass filter and a high pass filter (Fig 3). The low pass filter gives the approximations (A) which are described by the relation

$$y(n) = 1/2x(n) + 1/2x(n-1) \quad (1)$$

and the high pass filter gives the details (D) which are described by the relation

$$y(n) = 1/2x(n) - 1/2x(n-1) \quad (2)$$

Wavelet analysis enables us to de-noise the signal by using an automatic or a manual threshold. An example of 1st level decomposition of a signal constructed with Rbio wavelets in the environment of MATLAB is shown in Fig.4.

RESULTS AND DISCUSSION

Intermediate-wet porous medium

The transient response of the capillary pressure measured during an oil/water displacement in a homogeneous intermediate-wet porous medium ($f_p=0$) is shown in Fig.5. The details of the 1st level decomposition obtained with wavelet analysis are shown in Fig. 6. This diagram can be regarded as the capillary pressure spectrum of the displacement. The time required for water breakthrough to take place was 48000 sec whereas the mean pre-breakthrough capillary pressure was 87 Pa.

In Fig. 7, the area between the 500th and 1500th measurement of Fig.6 was magnified. Each peak in Fig.7 corresponds to an abrupt or gradual decrease of the capillary pressure,

associated with a sequence of flow events, occurring in some region of the porous medium and identified from successive snapshots (Fig.8). Several of the most important flow events, identified from the snapshots of the displacement, along with the corresponding response of the capillary pressure are illustrated in Figs.8-10.

The foregoing analysis was repeated for various peaks of the capillary pressure spectrum (Fig.7). In intermediate-wet porous media, respectable fluctuations of the capillary pressure may arise from three classes of flow events:

- 1) Growth of a capillary finger
- 2) Coalescence of two moving interfaces
- 3) Penetration of the invading fluid into a cluster of pores

Each class of flow events can easily be identified given that the corresponding decrease of the capillary pressure and the relevant time interval (Figs.8-10) have been determined. Specifically, it has been observed that $\Delta P_{C1} \gg \Delta P_{C2}$ and $\Delta t_1 \gg \Delta t_2$, whereas $\Delta t_2 \ll \Delta t_3$ even if $\Delta P_{C3} = \Delta P_{C2}$. Therefore the amplitude of the capillary pressure fluctuation along with the time interval within which this fluctuation takes place, provide all information required for the identification of the various flow events.

Fractional-wet porous medium

The transient response of the capillary pressure measured during the water/oil displacement in a fractional-wet porous medium ($f_p=0.59$) where the ow and iw particles are mixed randomly, is shown in Fig.11. A magnified area of the capillary pressure spectrum ($N=900-1900$) resulting from the wavelet analysis is shown in Fig.12. Each peak of Fig. 12 corresponds to a fluctuation of the capillary pressure, which, in turn, is associated with a sequence of flow events illustrated in the snapshots of the displacement (Fig. 12b,c,d). Each area of the porous medium that is invaded by the wetting fluid is characterized by a wettability factor F resulting from four component percentages:

$f_{iw-iw-iw}$: the percentage of iw-iw-iw pore chambers with respect to the total number of invaded chambers.

$f_{iw-iw-ow}$: the percentage of iw-iw-ow pore chambers with respect to the total number of invaded chambers.

$f_{iw-ow-ow}$: the percentage of iw-ow-ow pore chambers with respect to the total number of invaded chambers.

$f_{ow-ow-ow}$: the percentage of ow-ow-ow pore chambers with respect to the total number of invaded chambers.

The local wettability factor F is defined by

$$F = f_{iw-iw-iw} - \frac{1}{3} f_{iw-iw-ow} - \frac{2}{3} f_{iw-ow-ow} - f_{ow-ow-ow} \quad (3)$$

and can be regarded as an algebraic measure of the contribution fraction of the iw pores to the total number of invaded pores. For each class of flow events, identified from successive snap-shots of the displacement (Fig.13), this parameter is correlated with the magnitude of the decrease of the capillary pressure.

Evidently, an increase of the wettability factor F (or equivalently, an increase of the fraction of the intermediate-wet solid surface that is invaded by the wetting fluid) results in a higher decrease of the capillary pressure (Fig.13). This conclusion can be generalized only for flow events of the same category (e.g. capillary fingering, coalescence of moving interfaces, etc). Finally, it was found that the average pre-breakthrough capillary pressure increases linearly with the fraction of oil-wet particles (Figure 14).

Non-random fractional wettability

A mixed-wet porous medium was constructed by placing in series three layers of sphere packings of different wettability (Fig.15). The first layer was composed of intermediate-wet glass spheres, the second layer was composed of oil-wet PTFE spheres, and the third layer was a mixture of PTFE and glass spheres (Fig. 15). The corresponding transient response of the capillary pressure is shown in Fig.16. Depending on the area where menisci advancement occurs, five regions can be distinguished in the capillary pressure signal (Fig.16):

1. In the 1st region, the water penetrates into the intermediate-wet area of the porous medium.
2. In the 2nd region, the water penetrates into the intermediate-wet area of the porous medium although it has already reached the boundary between the intermediate-wet and oil-wet areas.
3. In the 3rd region, the water penetrates into the oil-wet area of the porous medium and forms a network spanning cluster of wetting fluid in this area.
4. In the 4th region, the water penetrates into the fractional-wet area of the porous medium.
5. In the 5th region breakthrough of water has occurred.

The 1st region of Fig.16 shows the fluctuations of the capillary pressure as the water penetrates in the intermediate-wet area of the model (Fig.17a). In this region, the maximum capillary pressure measured was **120 Pa**. As soon as water reaches the entrance of the oil-wet area, a higher capillary pressure is required for menisci to move inside it with result that the menisci prefer to keep moving within the intermediate-wet area (Fig.17b). In the 2nd region the maximum capillary pressure measured was **140 Pa**. When the capillary pressure exceeds the critical value required for menisci to penetrate in the throats of the oil-wet area, capillary fingers start growing in this area, while at the same time some oil is still displaced by water in the intermediate-wet area (Fig.17c). In the 3rd region, the maximum pressure drop measured was **150 Pa**. As soon as the water expels from the outlet of the oil-wet area, the capillary pressure is reduced (4th region), but it is still high enough to allow the motion of menisci in the fractional-wet area (Fig.17d).

After the oil breakthrough, the total pressure drop across the porous medium may be approximated by the following equation

$$\Delta P_{wt} = \frac{u_w \mu_w}{k} \left(\frac{\Delta x_1}{k_{rw1}} + \frac{\Delta x_2}{k_{rw2}} + \frac{\Delta x_3}{k_{rw3}} \right) + \langle P_{cf} \rangle \quad (4)$$

where $k_{rw1}, k_{rw2}, k_{rw3}$ are average water relative permeabilities over the three layers of thickness $\Delta x_1, \Delta x_2, \Delta x_3$ respectively, and $\langle P_{cf} \rangle$ is a frontal capillary pressure averaged over the entire pore network. As the displacement is quasi-static and is governed by capillary forces, the viscous term of the right-hand of Eq.(4) is much less than $\langle P_{cf} \rangle$. In this manner, the measured post-breakthrough $\Delta P_{wt}(t)$ becomes negligible whenever a continuous pathway of water spans the porous medium ($\langle P_{cf} \rangle \cong 0$) and increases respectably whenever the continuity of water is interrupted and a finite capillary resistance arise (Fig.16, 5th region). The final result is very sharp fluctuations of the pressure drop (Fig.16). Initially, the water forms a continuous pathway in the 3rd fractional-wet layer, $\langle P_{cf} \rangle$ decreases and $\Delta P_{wt}(t)$ is reduced abruptly (Fig.17e, I). As the inlet pressure has decreased, oil from the intermediate-wet layer may be displaced by injected water and imbibe the oil-wet area by occupying regions of high curvature (e.g. pore cusps and pendular rings). Under such conditions, the hydraulic continuity of the wetting fluid (water) may be lost because of local capillary instability, and this happens at the boundary of the oil-wet and fractional-wet layers (Fig.17e, II). In order to keep the water influx rate constant, the inlet pressure, and hence the measured $\Delta P_{wt}(t)$ increases sharply. The oil is displaced by water from the high curvature regions of the oil-wet layer to the neighboring fractional wet layer and expels along with water from the outlet, the water regains its hydraulic continuity, and subsequently $\Delta P_{wt}(t)$ decreases dramatically (Fig.17e, III).

The non-random distribution of the heterogeneous wettability over the porous medium is the driving force for the fluctuations of the pressure drop (Fig.18a) and the subsequent discontinuous production of oil pockets after the water breakthrough (Fig.18b). The outlets of the porous medium were connected to a system of capillary tubes and capacitometers that enabled us to monitor precisely the water and oil volumes outflowing. Although the wettability of the pore system, on average, remains identical, in this experiment, neither the continuity of water was interrupted, nor breakthrough of water occurred in the outlet connected to the pressure transducer. In this manner, after the water breakthrough, the $\langle P_{cf} \rangle$ is finite and hence the measured fluctuations of $\Delta P_{wt}(t)$ exhibit shorter and wider fluctuations, compared to those observed earlier (Fig.16). This non-uniqueness of the pressure drop response is associated with the great number of outlets. Because of the relatively small size of the porous medium, the fluctuations of the signal have the tendency to vanish as the number of outlets is reduced.

CONCLUSIONS

The fluctuations of the transient pressure drop that is measured during capillary-driven displacement experiments in transparent and fractional-wet model porous media is analyzed with wavelets in order to construct a spectrum of the capillary pressure fluctuations. These fluctuations are correlated with the various classes of flow events that are video-recorded with the aid of an image capturing system. The final goal is the

development of a method that will use the capillary pressure spectrum as a fingerprint of the fractional wettability of the porous medium. The most important conclusions are outlined below.

- Wavelet analysis produces a capillary pressure spectrum that enables us to quantify easily the position, maximum decrease and width of the capillary pressure fluctuations.
- The measured fluctuations of the capillary pressure can be correlated with a local wettability factor, only if they refer to the same class of flow events.
- The average pre-breakthrough capillary pressure is a linearly increasing function of the fraction of oil-wet particles.
- In cases of layered and non-randomly distributed fractional wettability, the post-breakthrough fluctuations of the capillary pressure are associated with the fluid transfer between areas of different wettability and the discontinuous recovery of oil pockets.

ACKNOWLEDGEMENTS

This work was performed under Global Change and Ecosystems contract number 004017 (GOCE)-STRESOIL (2004-2007) supported by the European Commission.

REFERENCES

1. Anderson, W. G., "Wettability literature survey-Part 2: wettability measurement", *J. Pet. Technol.* (1986) **Nov.**, 1246-1262.
2. Araujo, Y. C., and Araujo, M., "Geometrical description of contact angle line fluctuations in heterogeneous systems with controlled wettability", *J. Colloid Interface Sci.* (2000) **229**, 92-101.
3. Blunt, M. J., "Physically based network modeling of multiphase flow in intermediate wet porous media", *J. Petr. Sc. Eng.* (1998) **20**, 117-125.
4. Dominguez, A., Perez-Aguilar, H., Rojas, F., and Kornhauser, I., "Mixed wettability: a numerical study of the consequences of porous media morphology", *Colloids and Surfaces A: Phys. & Eng. Aspects* (2001) **187-188**, 415-424.
5. Guan, H., Brougham, D., Sorbie, K. S., and Packer, K. J., "Wettability effects in a sandstone reservoir and outcrop cores from NMR relaxation time distributions", *J. Pet. Sci. and Eng.* (2002) **34**, 35-54.
6. Hirasaki, G.J., "Wettability: fundamentals and surface forces", *SPEFE* (1991) **June**, 217-226.
7. Jackson, M.D., Valvatne, P. H., Blunt, M. J., "Prediction of wettability variation and its impact on flow using pore- to reservoir- scale simulations", *J. Petr. Sc. Eng.* (2003) **39**, 231-246.
8. Laroche, C., Vizika, O., Kalaydjian, F., "Network modeling as a tool to predict three-phase gas injection in heterogeneous wettability porous media", *J. Petr. Sc. Eng.* (1999) **24**, 155-168.
9. Mahrooqi, S. H., Grattoni, C. A., Moss, A. K., Jing, X. D., "An investigation of the effect of wettability on NMR characteristics of sandstone rock and fluid systems", *J. Petr. Science Engineering* (2003) **39**, 389-398.
10. Schramm, L. L., and Mannhardt, K., "The effect of wettability on foam sensitivity to crude oil in porous media", *J. Pet. Sci. and Eng.* (1996) **15**, 101-113.
11. Sharma, M. M. and Wunderlich, R. W., "The alteration of rock properties due to interaction with drilling fluid components", *J. Pet. Sci. Eng.* (1987) **1**, 127-143.
12. Tsakiroglou, C.D. and Fleury, M., "Resistivity index of fractional wettability porous media", *J. Pet. Sci. Eng.* (1999) **22**, 253-274.

13. Tsakiroglou, C.D., Theodoropoulou, M., Karoutsos, V., Papanicolaou, D., and Sygouni, V., "Experimental study of the immiscible displacement of shear-thinning fluids in pore networks", *J. Colloid Interface Science* (2003) **267**, 217-232.
14. Tzimas, G. C., Matsuura, T., Avraam, D. G., van der Bruggen, W., Constantinides, G.N., and Payatakes, A.C., "The combined effect of the viscosity ratio and the wettability during forced imbibition through nonplanar porous media", *J. Colloid Interface Sci.* (1997) **189**, 27-36.
15. Yuan, H. H., and Swanson, B.F., "Resolving pore-space characteristics by rate-controlled porosimetry", *SPEFE* (1989) **March**, 17-24.

Table 1. Physicochemical properties of fluids

Silicon oil density, ρ_o (Kg/m ³)	970
Silicon oil viscosity, μ_o (Pa s)	0.033
Deionized water density, ρ_w (Kg/m ³)	995
Deionized water viscosity, μ_w (Pa s)	10 ⁻³
Interfacial tension, γ_{ow} (N/m)	32.7 10 ⁻³
o/w contact angle on glass, θ_e (°)	60
o/w contact angle on PTFE, θ_e (°)	178

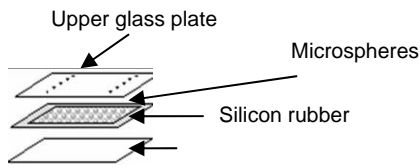


Figure 1. The model porous medium

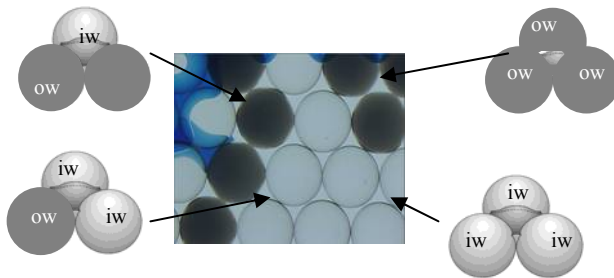


Figure 2. Various classes of pore chambers

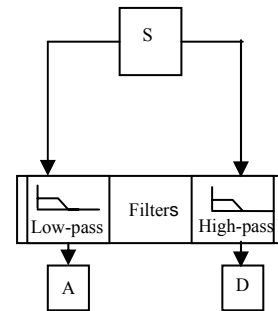


Figure 3. 1st level wavelet decomposition of a signal

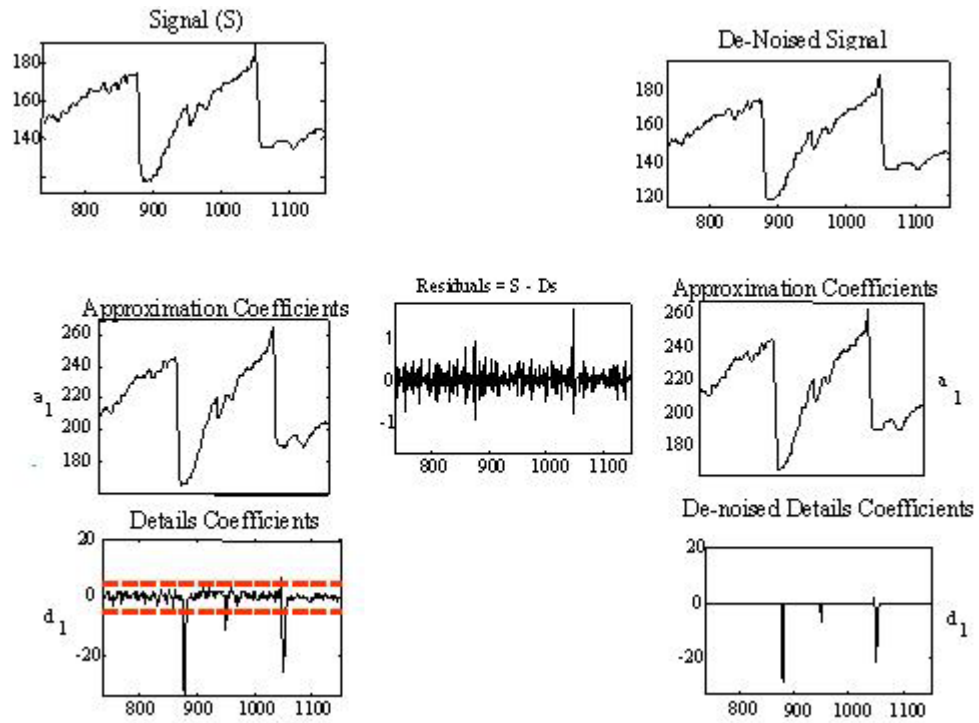


Figure 4. 1st level decomposition and de-noising of a signal with wavelets.

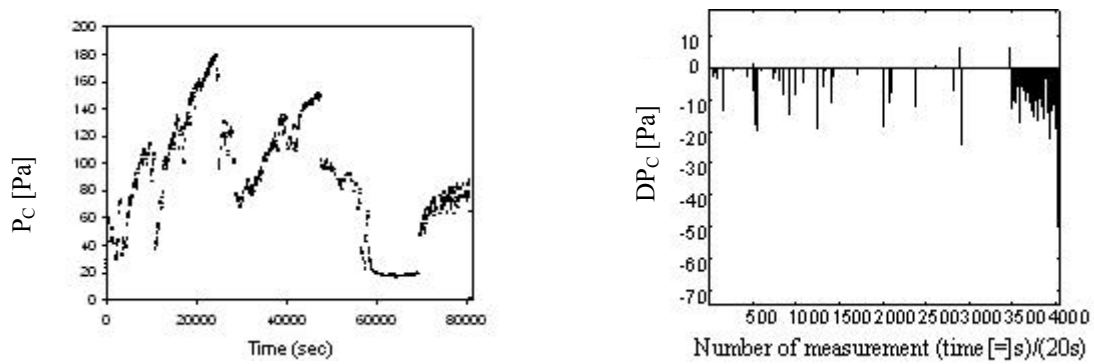


Figure 5. Original signal of the transient response of the capillary pressure for $f_p=0.0$

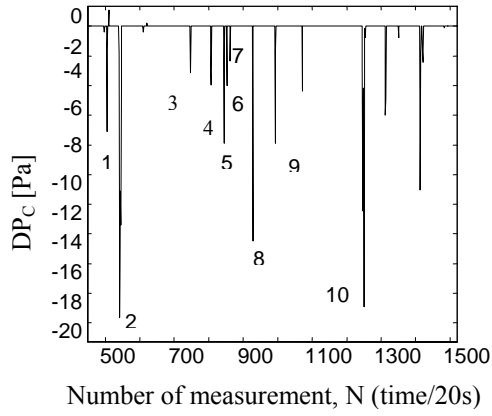


Figure 7. Magnification of an area of Fig.6

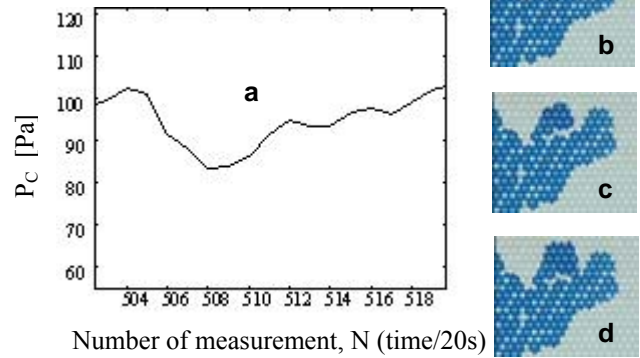


Figure 8. (a) The segment of the original signal where the maximum decrease of the pressure drop $\Delta P_C = -19.2$ Pa occurs at a time interval $\Delta t = 80.4$ s. It corresponds to peak 1 (Fig.7) with $DP_C = -7.12$ Pa. (b-d) Sequence of corresponding flow events: penetration of water in a cluster of pores and subsequent coalescence of interfaces.

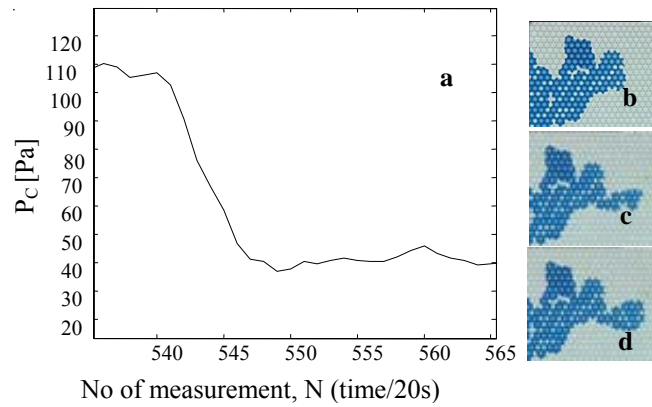


Figure 9. (a) The segment of the original signal where the maximum decrease of the capillary pressure $\Delta P_C = -73.6$ Pa occurs at a time interval $\Delta t = 261$ s. It corresponds to peak 2 (Fig.7) with $DP_C = -19.7$ Pa. (b-d) Sequence of corresponding flow events: growth of capillary fingers.

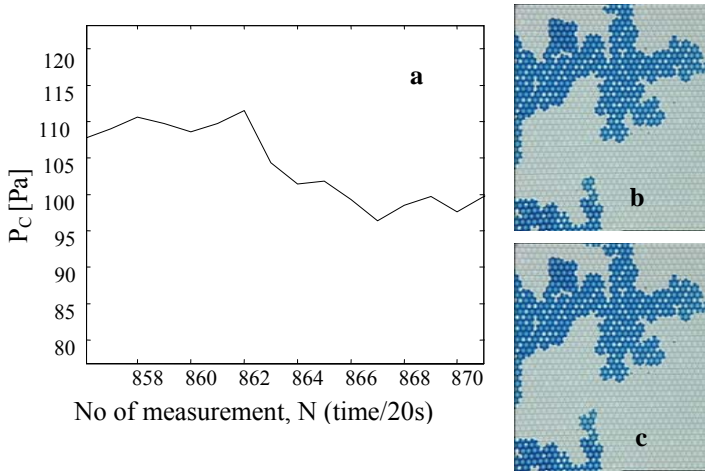


Figure 10. (a) The segment of the original signal where the maximum decrease of the capillary pressure $\Delta P_C = -15.3$ Pa occurs at a time interval $\Delta t = 99$ s. It corresponds to peak 7 (Fig.7) with $DP_C = -2.4$ Pa. (b-c) Sequence of corresponding flow events: penetration in a cluster of pores

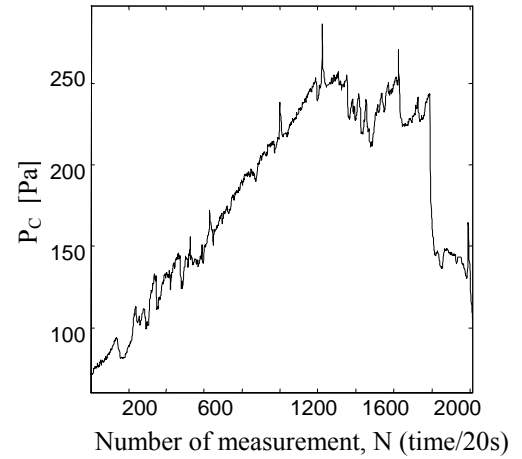


Figure 11. Original signal of the transient response of the pressure drop for $f_p = 0.59$

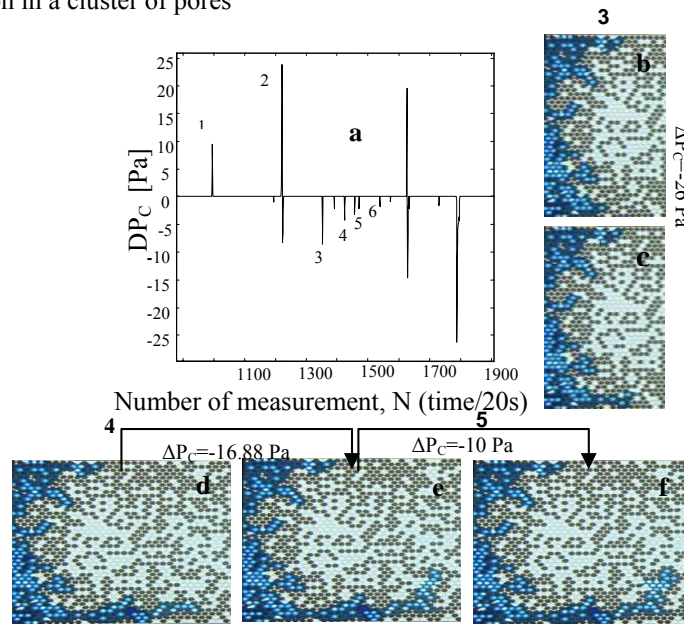


Figure 12. (a) A segment of the capillary pressure spectrum for $f_p = 0.59$. (b-c) Successive snapshots of the displacement that correspond to the capillary pressure decrease of the peak 3. (d-e) Successive snapshots of the displacement that correspond to the capillary pressure decrease of the peak 4. (e-f) Successive snapshots of the displacement corresponding to the capillary pressure decrease of the peak 5

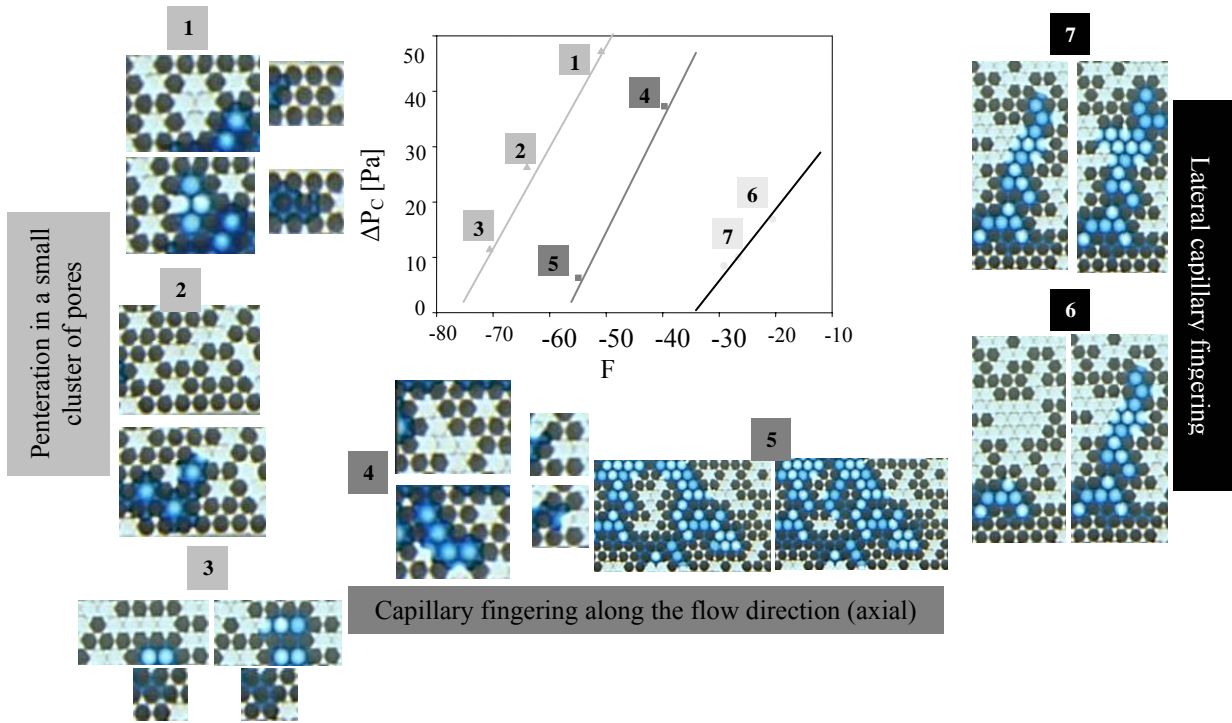


Figure 13. Decrease of the capillary pressure as a function of the wettability factor F for $f_p=0.59$. The corresponding flow events are also illustrated.

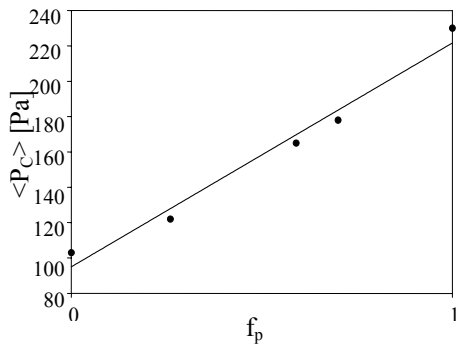


Figure 14. Average capillary pressure as a function of the fraction of oil-wet particles, f_p .

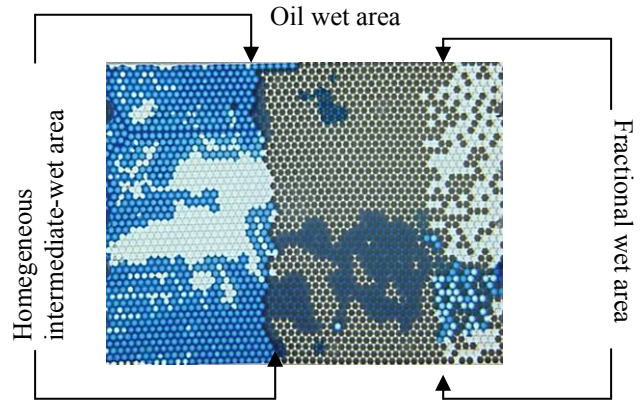


Figure 15. The three areas of different wettability

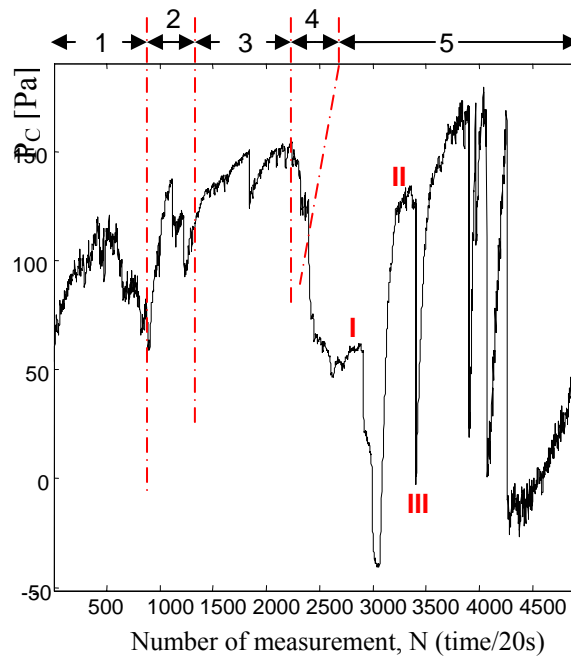


Figure 16. The five regions of the pressure drop signal

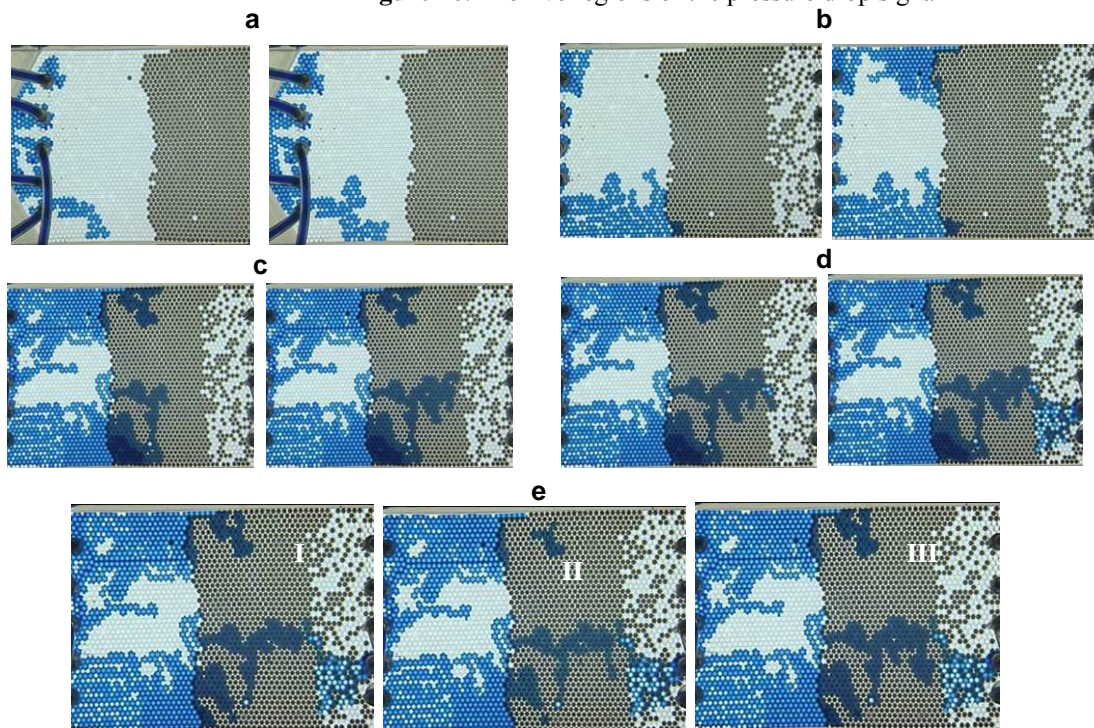


Figure 17. (a) Water penetration in the intermediate-wet area of the porous medium (1st region of Fig.16).
 (b) Water penetration in the intermediate-wet area while it has already reached the oil wet area of the porous medium (2nd region of Fig.16).
 (c) Water penetration in the oil wet area of the porous medium (3rd region of Fig.16).
 (d) Water penetration in the mixed wet area of the porous medium (4th region of Fig.16).
 (e) Snap shots of the displacement after breakthrough (points I, II and III of the 5th region of Fig.16).

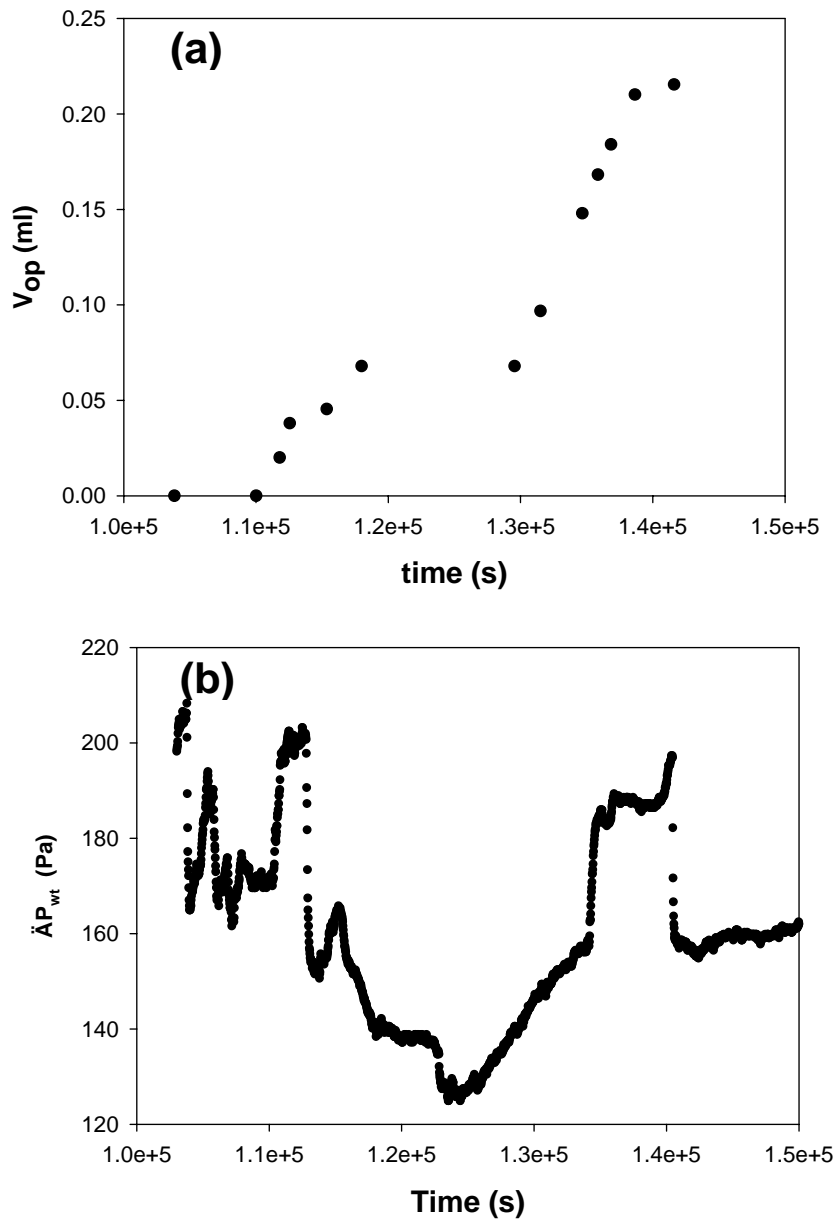


Figure 18. Post-breakthrough (a) oil produced as a function of time, (b) measured response of the pressure drop